

RESEARCH ARTICLE

[View Article Online](#)
[View Journal](#) | [View Issue](#)



Cite this: *Inorg. Chem. Front.*, 2025,
12, 980

Flexibility index: a general descriptor of polarization ability in crystalline materials†

Qin Chen, ^{a,c} Xingxing Jiang ^{*a} and Zheshuai Lin ^{*a,b,c}

Although optical phenomena in crystalline materials are different, they are all generated from the polarization processes of microscopic structural units under a photoelectric field. Thus, the development of simple and effective models that can evaluate the polarization ability of optical materials is crucial for their structural screening and mechanism analysis. Herein, we applied the “flexibility (*F*) index”, a model previously used to investigate the structural origin of second-order nonlinear optical responses in unitary and binary diamond-like materials. We demonstrated that this index has a negative correlation with their band gap and a positive correlation with their first- and second-order polarizabilities. Remarkably, the first-order polarizability showed a linear-function correlation with the *F*-index, while the second-order polarizability exhibited a cube-function correlation with the “projected-flexibility (*F*_p) index”. These polarizability-order-dependent correlations validated the feasibility of the *F*-index in characterizing specific optical properties. The results of this study prove the universality of the *F*-index to describe optical polarization, which serves as a quick and efficient tool to evaluate the optical response in crystalline materials.

Received 30th October 2024,
Accepted 8th December 2024
DOI: 10.1039/d4qi02749c
rsc.li/frontiers-inorganic

10th anniversary statement

I have been publishing articles in *Inorg. Chem. Front.* since 2015, and now, after 10 years, I am delighted to witness this journal ranking among the top three in the field of inorganic chemistry in the Journal Citation Reports (JCR) Q1 of Chinese Academy of Sciences (CAS). During the submission process, the editor processed this manuscript in a timely manner, and the comments by the reviewers were professional and pertinent, significantly improving the level of our research. I hope that this journal will continue to maintain its efficiency, cutting edge and professionalism and become a flagship academic journal that leads the development of inorganic chemistry internationally.

1. Introduction

Optical responses, such as refraction,¹ second harmonic generation (SHG),² two-photon absorption³ and Raman scattering,⁴ are ubiquitous and have been key concepts in both fundamental science and advanced engineering research. Although these optical responses in solids differ from one to another, their fundamental physics relies on an induced polarization under a photoelectric field, which can be mathematically described by the polarization equation, as follows:

$$P = P_0 + \chi^{(1)}E + \chi^{(2)}E^2 + \chi^{(3)}E^3 + \dots$$

^aFunctional Crystals Lab, Technical Institute of Physics and Chemistry, Chinese Academy of Sciences, Beijing 100190, China. E-mail: xxjiang@mail.ipc.ac.cn, zslin@mail.ipc.ac.cn

^bCenter of Materials Science and Optoelectronics Engineering, University of the Chinese Academy of Sciences, Beijing 100049, China

^cUniversity of the Chinese Academy of Sciences, Beijing 100049, China

† Electronic supplementary information (ESI) available. See DOI: <https://doi.org/10.1039/d4qi02749c>

where P and P_0 are the induced polarization with and intrinsic polarization without a photoelectric field, respectively, $\chi^{(n)}$ is the n -th polarizability, and E is the photoelectric field. Accordingly, optical responses are exclusively governed by the polarizabilities (i.e., $\chi^{(1)}, \chi^{(2)}, \chi^{(3)} \dots$). Rationally evaluating the polarization capability of materials is the key to understanding their optical properties, which has a long research history due to its great significance in disclosing the related mechanism and performance prediction.^{5,6} All the relevant studies to date can be roughly divided into two categories. First are those studies that benefitted from the development of computational software and computational algorithms, and a great deal of exact optical properties have been well computed by algorithms based on quantum chemistry,⁷ density functional theory (DFT),⁸ lattice dynamics,⁹ and the recently booming artificial intelligence.¹⁰ The second category is based on fundamental physical and chemical perspectives, and structural chemists and physicists are continuously searching for simple and feasible descriptors to characterize the polarization capability of materials.^{11–14} As a typical representative among them, the bond parameter method developed by Levine once served as the most

popular method to compute the nonlinear optical susceptibility.¹⁵ However, the large-scale simulation on the exact optical properties has strongly promoted the exploration of novel materials and mechanism elaboration, which is becoming the mainstream approach in the field of polarization-relevant materials. In this case, it is necessary to develop models that are as simple as possible and can grasp the most fundamental physics and chemistry of polarization, while still clearly helping researchers in the structure screening of a large number of alternative materials.

In our previous study, based on the bond valence theory, we proposed a “flexibility (*F*) index” model of chemical bonds in inorganic crystals and clarified that their nonlinear optical response arises from the compliance of their dipole in response to external perturbation from a photoelectric field, rather than the static dipole moment.¹⁶ Since the proposal of the *F*-index, it has been widely utilized in mechanism explanation and performance prediction in the field of nonlinear optical crystals.^{17–19} Given that only two parameters, the quantities of bond electrons and exerted Coulomb force, are considered in this model, we postulate that it will be a general descriptor for the polarization capacity, and besides the nonlinear optical response, other polarization-relevant optical properties can be explained and described by this model. Herein, unitary and binary inorganic crystals with diamond-like structures were chosen to verify this hypothesis. The selection of this crystal system is based on the consideration that the number of intrinsic bond parameters predominantly governs their polarization and other interfering components is low due to the two structural characterizations (with the representative structure of zinc sulfide displayed in Fig. 1), as follows: (1) only one type of bond is contained in the lattices of these crystals and (2) all the constituent atoms are four-fold coordinated with each other, and the spatial orientation of the bonds in the lattice are similar. According to our calculation, the *F*-index was shown to have a pronounced negative correlation with the band gaps and positive correlation with the fundamental optical properties, including refractive index, polarizability, and nonlinear optical coefficient. Our work confirms the capacity of the *F*-index model as a general descriptor of polarization response ability in inorganic crystalline materials.

2. Computational method

In total, 69 unitary and binary diamond-like semi-conductors and insulators screened from the Materials Project database

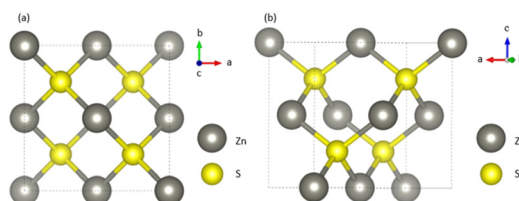


Fig. 1 Crystal structure viewed along (a) *c*- and (b) *b*-axis of the representative material zinc sulfide with a diamond-like structure.

were considered in this study.²⁰ The calculation of the refractive indices, polarizabilities, and SHG coefficients were implemented by DFT based on the plane-wave pseudopotential method,²¹ utilizing the CASTEP package.²² The Perdew–Burke–Ernzerhof (PBE) functionals in the form of the generalized gradient approximation (GGA)²³ were employed to describe the exchange and correlation terms in the Hamiltonian.²⁴ The electron–ion interactions were modeled using norm-conserving pseudopotential,²⁵ which allowed a relatively small plane-wave basis set without compromising the computational accuracy. A plane-wave basis set with an energy cutoff of 1000 eV and Monkhorst–Pack *k*-point grids with a spacing of less than 0.015 Å^{–1} in the Brillouin zone were adopted.²⁶ Prior to the property calculation, to get the theoretical optimal geometry configurations with the lowest energies, all the structures were optimized with both lattices and atomic positions relaxed by the Broyden–Fletcher–Goldfarb–Shanno (BFGS) scheme, with the convergence criteria of 5.0×10^{-6} eV per atom, 0.01 eV Å^{–1}, 0.02 GPa, and 5.0×10^{-4} Å for energy, maximum force, maximum stress and maximum displacement, respectively.²⁷

By considering that the band gaps are often underestimated by standard functionals,²⁸ scissor operators were used to raise the conduction bands (CB) to match the calculated band gaps with the experimental values.²⁹ Based on the scissor-operator-corrected band structures, the imaginary part of the dielectric function can be calculated from the matrix elements of the electronic transitions from the valence band (VB) to CB, and the real part of the dielectric function, *i.e.*, refractive index, could be determined using the Kramers–Kronig transformation.³⁰ The SHG coefficients were calculated using the formula in length-gauge developed by our group.³¹ The static (*f* ~ 0) and optical (*f* ~ ∞) polarizabilities were calculated using the linear response method.³² In the linear response algorithm, for an insulating system, polarization is computed by the derivative of the total energy with respect to a given perturbation of electric field, and further the polarizability can be obtained by differentiating the polarization with respect to the exerted electric field.

The formula to calculate the *F*-index is expressed as follows:¹⁶

$$F = \frac{\exp[(R_0 - R)/B]}{(\sqrt{C_a} + \sqrt{C_b})^2/R^2} \quad (1)$$

where the numerator represents the bond valence charge derived from the bond valence model,³³ in which *R* is the length of the concerned bond, *R*₀ is the ideal bond length when the bonding atoms perfectly contribute a unit valence,³⁴ and *B* is an empirical constant (typically 0.37 Å).³⁵ *C*_a and *C*_b are the charges of the atomic cores formed by the bonding atoms losing the outer-shell electrons.

The even-order polarizability magnitude depends on the bond orientation governed by macroscopic symmetry,³⁶ which is exemplified by the fact that SHG coefficients are completely zero in the centrosymmetric lattice with large odd-order polarizability. To account for the contribution of the bond orien-

tations, a “projected flexibility (F_p) index” was calculated using the following formula:

$$F_p = \frac{\sum_{i=1}^n F_i \cos \theta_i}{n} \quad (2)$$

where F_i is the F -index of the i -th bond calculated using formula (1). θ_i is the angle between the i -th bond and the highest-order symmetric element of the lattice.

3. Results and discussion

Three macroscopic symmetries with the space groups, namely, $F\bar{d}3m$ (for diamond, silicon and germanium), $F\bar{4}3m$ (for zinc blende structures) and $P6_3mc$ (for wurtzite structures) were included in these 69 structures. All the discussed data are listed in Table S1.[†]

Firstly, the band gap was the focus, given that it is the most crucial and general parameter determining the optical properties in a crystal.³⁷ By considering that the band gaps cannot be well theoretically reproduced by one universal functional for all the investigated structures with their experimental

values spanning a wide range (0.66 eV–10.6 eV), here the experimental values (listed in Table S1[†]) were directly used for correlation with the F -index. As plotted in Fig. 2, a pronounced negative correlation was observed for the dependence of the band gap on the F -index, with a small confidence interval (less than 1.94 eV) for the confidence value of 95%. The band gap characterizes the energy barrier that an electron in the bound state needs to overcome to transit to the free state.³⁸ In the formula of the F -index, the denominator describes the binding force exerted on the unit bond charge from the bonding atoms, coincidentally corresponding to the force in the classical sense that an electron should overcome to escape from the bond constraint. The negative correlation between these two quantities intuitively indicates that the band gap engineering lies in the regulation of the binding force of the valence electrons from the lattice by controlling parameters such as the atomic valence state and radius. The negative correlation between the F -index and band gap gives confidence to further discuss the exact optical properties.

Now, we focused on the optical properties relevant to the first-order polarizability. Fig. 3a shows the dependence of the calculated refractive indices (values at the wavelength of 1 μm) on F -index. It can be seen that the refractive indices positively depend on the values of the F -index, and a linear dependence with the confidence interval less than 0.45 for the confidence value of 95% can be fitted. More finely, positive correlations are clearly observed for the three branch systems separately as well. The static (frequency, $f \sim 0$) polarizability and the polarizability at optical frequencies limit ($f \sim \infty$) are shown in Fig. 3b and c, respectively, and the evident increasing tendencies of the polarizabilities *versus* F -index are observed as well. In the polarizability calculation by the linear response method,³² besides the electron contribution, the contribution from atomic cores (*i.e.*, phonon) is involved. It should be that in the F -index model,¹⁶ the bonding electrons are bound by the atoms, and conversely the bonded atoms are bound by the bonding electrons *via* the same force as well. From this perspective, actually, the atomic contribution is also included in the F -index, and the F -index can also characterize the magnitude of atomic displacement under the perturbation of an

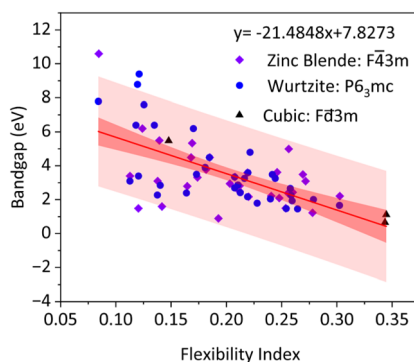


Fig. 2 Distribution of experimental band gaps versus F -index. The dark and light red regions represent the 95% confidence interval and 95% prediction interval, respectively.

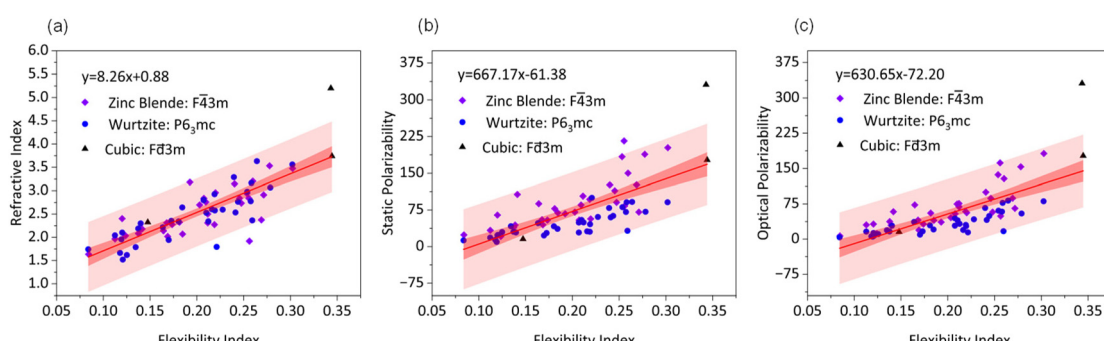


Fig. 3 Distributions of (a) refractive indices, (b) static polarizabilities and (c) optical-frequency polarizabilities versus F -index. The dark and light red regions represent the 95% confidence intervals and 95% prediction intervals, respectively.

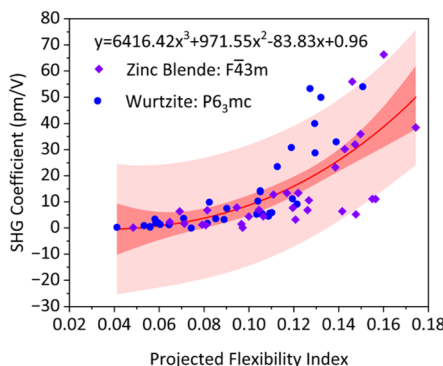


Fig. 4 Distribution of SHG coefficients versus F_p -index. The dark and light red regions represent the 95% confidence interval and 95% prediction interval, respectively.

exerted photoelectric field. The prominent positive linear correlations between the F -index and refractive index, static polarizability and optical-frequency polarizability validate the feasibility of the F -index in describing the first-order polarizability.

Given that even-order polarizability is forbidden in centrosymmetric structures,³⁹ in the case of the SHG coefficient, only the non-centrosymmetric zinc blende and wurtzite materials were the focus here. By considering that the macroscopic SHG response depends on the bond orientation in the lattice,⁴⁰ here, a “projected flexibility (F_p) index”, the average values of the projection of the F -index onto the highest symmetric elements (four-fold axes for zinc blende and six-fold axes for wurtzite, respectively) in the constitute bonds are used. Fig. 4 shows the variation of the calculated SHG coefficients versus F_p -index, and accordingly, an increasing tendency is also observed. It should be noted that different from the band gap and first-order polarizabilities described by the linear relation, the dependence of the SHG coefficients on the F_p -index is well fitted by a cubic function. The SHG response is a second-order polarization process in a crystal, and according to the Miller rule derived from the Lorentz model based on the anharmonic perturbation theory,^{41,42} the second-order nonlinear susceptibility is proportional to the cube of the refractive index in a material. The cube correlation between F_p -index and SHG coefficient is well consistent with the conclusion deduced in the Lorentz model, which verifies the description of the F_p -index on the second-order polarizability.

4. Conclusion

In summary, to generally model the photoelectric-field polarization capacity in crystalline materials, the F -index based on the bond valence theory, which was previously used to clarify the origin of the second-order nonlinear optical response, was utilized to relate the polarizability in unitary and binary diamond-like materials. The negative correlation between the experimental band gaps and F -index verified the general feasibility of the latter to grasp the fundamental essence of the

polarization process. The fitted linear positive correlation between the F -index and first-order polarizability, including refractive index, static polarizability and optical-frequency polarizability, confirmed the capacity of the F -index to qualitatively describe the exact optical properties. Moreover, to account for the role of the bond orientation in determining the macroscopic second-order polarizability, the F_p -index was proposed. Its cube correlation with the SHG coefficients agreed with the conclusion deduced from the Miller rule, further verifying its applicability to (semi-) quantitatively evaluate the polarizability. This work provides a simple and effective descriptor to universally model the polarization process and evaluate the polarizability in crystalline materials, which can be used to perform quick structure–screening and structure–property relation analysis, and then help promote studies on polarization-relevant functional materials.

Data availability

The data that support the findings of this study are available in the ESI† of this article.

Conflicts of interest

The authors declare that they have no known competing financial interests or personal relationships that could have appeared to influence the work reported in this paper.

Acknowledgements

This work was supported by the National Natural Science Foundation of China (grants T2222017, 12274425, 22375211, 22133004 and 22421005) and the CAS Project for Young Scientists in Basic Research (YSBR-024).

References

- 1 M.-H. Lu, C. Zhang, L. Feng, J. Zhao, Y.-F. Chen, Y.-W. Mao, J. Zi, Y.-Y. Zhu, S.-N. Zhu and N.-B. Ming, Negative birefraction of acoustic waves in a sonic crystal, *Nat. Mater.*, 2007, 6, 744–748.
- 2 Z. Yan, J. Fan, S. Pan and M. Zhang, Recent advances in rational structure design for nonlinear optical crystals: leveraging advantageous templates, *Chem. Soc. Rev.*, 2024, 53, 6568–6599.
- 3 F. Helmchen and W. Denk, Deep tissue two-photon microscopy, *Nat. Methods*, 2005, 2, 932–940.
- 4 S. Wu, F.-T. Huang, X. Xu, E. T. Ritz, T. Birol, S.-W. Cheong and G. Blumberg, Polar charge density wave in a superconductor with crystallographic chirality, *Nat. Commun.*, 2024, 15, 9276.

5 V. Dimitrov and T. Komatsu, Classification of simple oxides: A polarizability approach, *J. Solid State Chem.*, 2002, **163**, 100–112.

6 S. L. Price, M. Leslie, G. W. A. Welch, M. Habgood, L. S. Price, P. G. Karamertzanis and G. M. Day, Modelling organic crystal structures using distributed multipole and polarizability-based model intermolecular potentials, *Phys. Chem. Chem. Phys.*, 2010, **12**, 8478–8490.

7 B. J. Wieder, B. Bradlyn, J. Cano, Z. Wang, M. G. Vergniory, L. Eleoro, A. A. Soluyanov, C. Felser, T. Neupert, N. Regnault and B. A. Bernevig, Topological materials discovery from crystal symmetry, *Nat. Rev. Mater.*, 2022, **7**, 196–216.

8 L.-P. Miao, N. Ding, N. Wang, C. Shi, H.-Y. Ye, L. Li, Y.-F. Yao, S. Dong and Y. Zhang, Direct observation of geometric and sliding ferroelectricity in an amphidynamic crystal, *Nat. Mater.*, 2022, **21**, 1158–1164.

9 J. Vodeb, M. Diego, Y. Vaskivskyi, L. Logaric, Y. Gerasimenko, V. Kabanov, B. Lipovsek, M. Topic and D. Mihailovic, Non-equilibrium quantum domain reconfiguration dynamics in a two-dimensional electronic crystal and a quantum annealer, *Nat. Commun.*, 2024, **15**, 4836.

10 A. Leitherer, B. C. Yeo, C. H. Liebscher and L. M. Ghiringhelli, Automatic identification of crystal structures and interfaces via artificial-intelligence-based electron microscopy, *npj Comput. Mater.*, 2023, **9**, 179.

11 S. Miyahara and N. Furukawa, Theory of antisymmetric spin-pair-dependent electric polarization in multiferroics, *Phys. Rev. B*, 2016, **93**, 014445.

12 X. Zhao and X. Wang, A novel strategy for comprehensive estimation of lattice energy, bulk modulus, chemical hardness and electronic polarizability of $A^N B^{8-N}$ binary inorganic crystals, *Crystals*, 2023, **13**, 668.

13 P. Politzer, P. Jin and J. S. Murray, Atomic polarizability, volume and ionization energy, *J. Chem. Phys.*, 2002, **117**, 8197–8202.

14 V. V. Atuchin, B. I. Kidyarov and N. V. Pervukhina, Phenomenological modeling and design of new acentric crystals for optoelectronics, *Comput. Mater. Sci.*, 2004, **30**, 411–418.

15 B. F. Levine, Bond-charge calculation of nonlinear optical susceptibilities for various crystal structures, *Phys. Rev. B*, 1973, **7**, 2600–2626.

16 X. Jiang, S. Zhao, Z. Lin, J. Luo, P. D. Bristowe, X. Guan and C. Chen, The role of dipole moment in determining the nonlinear optical behavior of materials: Ab initio studies on quaternary molybdenum tellurite crystals, *J. Mater. Chem. C*, 2014, **2**, 530–537.

17 R. Wang, F. Liang and Z. Lin, Data-driven prediction of diamond-like infrared nonlinear optical crystals with targeting performances, *Sci. Rep.*, 2020, **10**, 3486.

18 S. Yang, C. Lin, H. Fan, K. Chen, G. Zhang, N. Ye and M. Luo, Polar Phosphorus Chalcogenide Cage Molecules: Enhancement of Nonlinear Optical Properties in Adducts, *Angew. Chem., Int. Ed.*, 2023, **62**, e202218272.

19 L. Wu, H. Tian, C. Lin, X. Zhao, H. Fan, P. Dong, S. Yang, N. Ye and M. Luo, Optimized arrangement of non- π -conjugated PO_3NH_3 units leads to enhanced ultraviolet optical nonlinearity in $NaPO_3NH_3$, *Inorg. Chem. Front.*, 2024, **11**, 1145–1152.

20 A. Jain, J. Montoya, S. Dwaraknath, N. E. R. Zimmermann, J. Dagdelen, M. Horton, P. Huck, D. Winston, S. Cholia, S. P. Ong and K. Persson, The materials project: Accelerating materials design through theory-driven data and tools, in *Handbook of Materials Modeling: Methods: Theory and Modeling*, 2018, pp. 1–34.

21 W. Kohn, Nobel lecture: Electronic structure of matter—wave functions and density functionals, *Rev. Mod. Phys.*, 1999, **71**, 1253–1266.

22 S. J. Clark, M. D. Segall, C. J. Pickard, P. J. Hasnip, M. I. J. Probert, K. Refson and M. C. Payne, First-principles methods using CASTEP, *Z. Kristallogr.*, 2005, **220**, 567–570.

23 J. P. Perdew, K. Burke and M. Ernzerhof, Generalized gradient approximation made simple, *Phys. Rev. Lett.*, 1996, **77**, 3865–3868.

24 J. P. Perdew, J. A. Chevary, S. H. Vosko, K. A. Jackson, M. R. Pederson, D. J. Singh and C. Fiolhais, Atoms, molecules, solids, and surfaces: Applications of the generalized gradient approximation for exchange and correlation, *Phys. Rev. B: Condens. Matter Mater. Phys.*, 1992, **46**, 6671–6687.

25 D. R. Hamann, Optimized norm-conserving vanderbilt pseudopotentials, *Phys. Rev. B: Condens. Matter Mater. Phys.*, 2013, **88**, 085117.

26 H. J. Monkhorst and J. D. Pack, Special points for brillouin-zone integrations, *Phys. Rev. B*, 1976, **13**, 5188–5192.

27 B. G. Pfrommer, M. Côté, S. G. Louie and M. L. Cohen, Relaxation of crystals with the quasi-newton method, *J. Comput. Phys.*, 1997, **131**, 233–240.

28 V. V. Turovtsev, Yu. D. Orlov and I. A. Kaplunov, Comparison of standard functionals to calculate the properties of molecules at the variational limit, *J. Struct. Chem.*, 2018, **59**, 1960–1966.

29 R. W. Godby, M. Schlüter and L. J. Sham, Self-energy operators and exchange-correlation potentials in semiconductors, *Phys. Rev. B: Condens. Matter Mater. Phys.*, 1988, **37**, 10159–10175.

30 J. Hong, A. Stroppa, J. Íñiguez, S. Picozzi and D. Vanderbilt, Spin-phonon coupling effects in transition-metal perovskites: A DFT + U hybrid-functional study, *Phys. Rev. B: Condens. Matter Mater. Phys.*, 2012, **85**, 054417.

31 J. Lin, M.-H. Lee, Z.-P. Liu, C. Chen and C. J. Pickard, Mechanism for linear and nonlinear optical effects in β - Ba_2O_4 crystals, *Phys. Rev. B: Condens. Matter Mater. Phys.*, 1999, **60**, 13380–13389.

32 M. Baldovin, F. Cecconi and A. Vulpiani, Understanding causation via correlations and linear response theory, *Phys. Rev. Res.*, 2020, **2**, 043436.

33 D. Brown, The chemical bond in inorganic chemistry: The bond valence model, in *The Chemical Bond in Inorganic Chemistry: The Bond Valence Model*, 2001.

34 G. Maroulis, Hyperpolarizability of H_2O , *J. Chem. Phys.*, 1991, **94**, 1182–1190.

35 N. E. Brese and M. O'Keeffe, Bond-valence parameters for solids, *Acta Crystallogr., Sect. B: Struct. Sci.*, 1991, **47**, 192–197.

36 L. Kim and T. Head-Gordon, Near equivalence of polarizability and bond order flux metrics for describing covalent bond rearrangements, *Phys. Chem. Chem. Phys.*, 2024, **26**, 27459–27465.

37 R. Woods-Robinson, Y. Han, H. Zhang, T. Ablekim, I. Khan, K. A. Persson and A. Zakutayev, Wide Band Gap Chalcogenide Semiconductors, *Chem. Rev.*, 2020, **120**, 4007–4055.

38 X. Ji, C. Lu, Z. Yan, L. Shan, X. Yan, J. Wang, J. Yue, X. Qi, Z. Liu, W. Tang and P. Li, A review of gallium oxide-based power Schottky barrier diodes, *J. Phys. D: Appl. Phys.*, 2022, **55**, 443002.

39 C. Chen, N. Ye, J. Lin, J. Jiang, W. Zeng and B. Wu, Computer-assisted search for nonlinear optical crystals, *Adv. Mater.*, 1999, **11**, 1071–1078.

40 M. Mutailipu, K. R. Poeppelmeier and S. Pan, Borates: A Rich Source for Optical Materials, *Chem. Rev.*, 2021, **121**, 1130–1202.

41 C. M. Bender and T. T. Wu, Large-order behavior of perturbation theory, *Phys. Rev. Lett.*, 1971, **27**, 461–465.

42 S. Scandolo and F. Bassani, Miller's rule and the static limit for second-harmonic generation, *Phys. Rev. B: Condens. Matter Mater. Phys.*, 1995, **51**, 6928–6931.